Hydrol. Earth Syst. Sci. Discuss., 10, 4015–4061, 2013
www.hydrol-earth-syst-sci-discuss.net/10/4015/2013/
doi:10.5194/hessd-10-4015-2013

Hydrology and Earth System Sciences
Open Access
Discussions

Optimising predictor domains for spatially coherent precipitation downscaling

S. Radanovics[1], J.-P. Vidal[1], E. Sauquet[1], A. Ben Daoud[2], and G. Bontron[2]

[1]Irstea, UR HHLY, Hydrology-Hydraulics Research Unit, 5 rue de La Doua, 69100 Villeurbanne, France
[2]Compagnie Nationale du Rhône (CNR), 2 rue André Bonin, 69316, Lyon Cedex 04, France

Received: 18 March 2013 – Accepted: 21 March 2013 – Published: 2 April 2013

Correspondence to: S. Radanovics (sabine.radanovics@irstea.fr)

Published by Copernicus Publications on behalf of the European Geosciences Union.

Abstract

Statistical downscaling is widely used to overcome the scale gap between predictors from Numerical Weather Prediction (NWP) models or General Circulation Models (GCMs) and predictands like local precipitation, required for example for medium-term operational forecasts or climate change impact studies. The predictors are considered over a given spatial domain which is rarely optimised with respect to the target predictand location. In this study the geopotential predictor domains used by an analogue downscaling method are optimised for 608 target zones covering France. An extended version of the growing rectangular domain algorithm provides an ensemble of five near-optimum domains for each target zone. All five near-optimum domains are consistently equally skillful based on the Continuous Rank Probability Score. Relevance maps calculated for selected target zones first reveal high skill geopotential regions with specific shapes for locations in south-eastern France compared to the rest of the country. In all cases, the optimised domains tend to include the most relevant area on the relevance maps. The domain centers of the optimised domains are mainly distributed following the geographical location of the target location, but there are apparent differences between the windward and the lee side of mountain ridges. Moreover, domains for target zones located in south-eastern France are centered more east and south than the ones for target locations on the same longitude. The size of the optimised domains tends to be larger in the southeastern part of the country, while domains with a very small meridional extent can be found in a east-west band around 47° N. Sensitivity tests on the archive length for the analogue method show a general robustness except for zones with high interannual variability like in the Cévennes area. Moreover, results appear to be rather unsensitive to the starting point of the optimisation algorithm except for zones located in the transition area north of the zones having optimized domains with a small meridional extent. This study paves the way for defining regions with homogeneous geopotential predictor domains for precipitation downscaling over France.

HESSD

10, 4015–4061, 2013

1 Introduction

For both climate change impact studies and operational hydrological forecasts precipitation information on the scale of small subcatchments is needed. Numerical Weather Prediction (NWP) models and General Circulation Models (GCMs) provide relevant information about the atmospheric large scale circulation but have too coarse resolution to be directly used in impact models like hydrological models or for precipitation forecasts on the scale of small subcatchments. A downscaling step is therefore required, and this can be done dynamically, using regional climate models and limited area models or using statistical methods that make use of statistical relationships between large-scale predictors and local-scale predictands.

Requirements for hydrological use of predictands specifically include the spatial coherence of precipitation fields over potentially large basins. Indeed, the generation of floods is for example particularly sensitive to the spatial distribution of precipitation over the catchment considered. When dynamical downscaling methods naturally provide such a sought-after spatial coherence, it is not necessarily the case for statistical methods. This paper therefore attempts to address this issue by considering an analogue downscaling method with more than 600 target zones covering the whole of France. A number of statistical downscaling studies with various methods have been performed over France over the last few years, but mainly on specific regions like the French Mediterranean (e.g. Quintana Seguí et al., 2010, 2011; Lavaysse et al., 2012; Kallache et al., 2011; Carreau and Vrac, 2011; Nuissier et al., 2011; Beaulant et al., 2011), Western France (e.g. Timbal et al., 2003), the French Alps (e.g. Martin et al., 1997) or the Seine basin (e.g. Boé et al., 2006). Until the present study, only a few of them have been performed at the country scale (Boé and Terray, 2008; Boé et al., 2009).

HESSD
10, 4015–4061, 2013

1.1 Statistical downscaling methods

In statistical downscaling a relationship between large scale predictors provided by GCMs and local scale predictands is established. There are three major groups of statistical downscaling methods used in a climate change context: model output statistics (MOS) (e.g. Chandler, 2002; Friederichs and Hense, 2007; Vidal and Wade, 2008; Lavaysse et al., 2012), Perfect Prognosis (PP) (e.g. Timbal et al., 2003; Boé et al., 2006; Hertig et al., 2012) and weather generators (e.g. Vrac et al., 2007; Chen et al., 2010; Bellone et al., 2000). A review of methods and their strengths and weaknesses to produce relevant input for impact models can be found in Maraun et al. (2010). Both PP and MOS methods are also applied for operational precipitation forecast (e.g. Marty et al., 2008, 2012, 2013; Voisin et al., 2010; Nam et al., 2011; Liu and Coulibaly, 2011; Muluye, 2011).

The downscaling method used in this work follows an analogue approach. The analogue method belongs to the PP methods and is based on the idea that similar causes have similar effects, i.e. similar predictor fields lead to similar predictand values. The analogue principle was introduced in forecasting by Lorenz (1969). Today numerous variants using different types of predictor fields and distance measures are in use. They range from weather typing-based methods based on principal components of mean sea level pressure fields (Boé et al., 2006) to MOS-like techniques based on precipitation field analogues (Hamill and Whitaker, 2006; Turco et al., 2011). A description of the theory of probabilistic forecasts with analogues can be found in Hamill and Whitaker (2006).

Analogue methods have been applied in different regions of the world with very diverse climates, e.g. Switzerland (Horton et al., 2012a), Australia (Timbal and McAvaney, 2001), central Sweden (Wetterhall et al., 2005), Punjab (India) (Raje and Mujumdar, 2011), south-east USA (Zhang and Georgakakos, 2012), the Alpine region (Themeßl et al., 2011), and north-east Spain (Ibarra-Berastegi et al., 2011).

HESSD
10, 4015–4061, 2013

1.2 Predictor domains: spatial variability and optimisation

The predictor variables used for statistical downscaling and the predictor domains have to be chosen carefully. The predictor variables should have predictive skill for the quantity to predict, here precipitation, they should be quantities that are reliably simulated by GCMs and ideally they should be related to the processes leading to precipitation and this relationships should persist in a changing climate (Wilby et al., 1998). When analogue methods are applied, only one predictor domain for all target locations is generally used, because this ensures that the same analogue dates will be selected for the whole region and this naturally leads to spatial coherence of the precipitation field. But for large target regions like whole France or large catchments with diverse precipitation climates like the Rhône basin this will likely result in less skill for smaller subcatchments.

In this study an analogue method is applied over the whole of France, which was rarely done so far and if so, using only one (Boé and Terray, 2008) or two (Timbal et al., 2003) different predictor domains and assuming that the same predictor domains are valid for large target regions. Here we will test if this assumption is valid by looking at predictor domains for different locations in France.

Additionally, in many downscaling studies no optimisation of the predictor domains is performed (Gutiérrez et al., 2013). Some tested a few different domains, for example Timbal and McAvaney (2001) who found that choosing an informative predictor domain is an important issue for the analogue selection. Ben Daoud (2010) found that some predictors like temperature or moisture variables have their main influence close to the target location and therefore a small predictor domain close to the target location is likely to be sufficient but the predictor domains for the shape of the geopotential field are usually larger and their optimum location depends on the meteorological situations that lead to precipitation at the target location. Bontron (2004) optimised the geopotential predictor domains for individual groups of precipitation station located in France and northern Italy and for all groups together and compared the performance difference for

HESSD
10, 4015–4061, 2013

different groups. For the groups near the center the difference was small, but groups far from the center benefit from individual predictor domains. Further he suggested to use the same predictor domain for groups situated not more than 250 km apart from each other and not separated by a major "climatological barrier".

Various algorithms may be used to optimise predictor domains. Ideally all predictor variables, predictor domains and other parameters should be optimised together and predictor domains of any size and shape should be possible. This was done by Sauter and Venema (2011) for an artificial neural network downscaling method and one target location in the Rhineland (Germany). Large computer ressources were needed to do so, because the search space is huge. Another interesting approach are genetic algorithms to optimise predictor domains Horton et al. (e.g. 2012b, for some stations in the Swiss Alps) but they have substantial computational costs as well. With the extended growing rectangular domains algorithm used in this work, the computational costs are comparatively low because the optimisation is restricted to geopotential predictor domains. This allows optimising domains for a large number of target zones separately, but also to obtain an ensemble of near-optimum domains for each target zone (see Sect. 2.5).

The work presented here builds upon a downscaling method that has a long history of development with various applications, like hydrological forecasts (Ben Daoud et al., 2011b) or historical flood reconstruction (Auffray et al., 2011). This analogue downscaling method will be used here to answer the following question: is the assumption made for example by Timbal et al. (2003) and Boé and Terray (2008) of a unique common predictor domain for large regions in France actually valid? To this aim, an ensemble of near-optimum geopotential predictor domains are derived for 608 target zones covering the whole of France. Sensitivity tests are furthermore performed to check the robustness of findings with respect to (1) the archive length, (2) the version of the optimisation algorithm and (3) the optimisation starting point.

HESSD
10, 4015–4061, 2013

The methods used for downscaling and optimisation are described in Sect. 2, results and sensitivity tests are described in Sect. 3, choices are discussed in Sect. 4 and conclusions are given in Sect. 5.

2 Data and methods

2.1 Data

2.1.1 Reanalyses

The predictor domain optimisation is done using two archives of reanalysis data. For the large scale ERA-40 data (Uppala et al., 2005) at 2.5° resolution is used. ERA-40 was chosen because of the trade off between archive length and data assimilation technique. The NCEP/NCAR reanalysis (Kalnay et al., 1996) has a longer archive but ERA-40 made use of the more advanced three dimensional variational data assimilation. Ben Daoud et al. (2009) compared ERA-40 and NCEP/NCAR reanalysis as large scale predictors for the analogue method and found slightly higher skill using ERA-40. ERA-Interim (Dee et al., 2011) uses an even more advanced data assimilation technique (4DVAR) but has still a shorter archive than ERA-40. Moreover, ERA-40 data is used as first guess for computing vertical profiles of near-surface variables by Safran.

Safran (French near surface reanalysis) data (Vidal et al., 2010) are used for the local daily precipitation which is the target variable addressed by the downscaling. The Safran reanalysis data are defined on 608 climatologically homogeneous zones covering France. Inside these zones the meteorological variables are supposed to depend only on altitude. These zones are used as elementary units in this work and are shown in Fig. 1. The algorithm used for the Safran analysis, its validation and its application over France are described by Quintana-Seguí et al. (2008). A detailed validation of this 50 yr atmospheric reanalysis over France has been carried out by Vidal et al. (2010). Of particular interest to this study, they found that the reanalysis uncertainty on

HESSD
10, 4015–4061, 2013

precipitation is both very low and relatively constant over the 1958–2008 period when considering both dependent and independent validation data. The bias calculated with 83 high-quality independent validation stations is smaller than 0.1 mm day^{-1} and the RMSE around 2.5 mm day^{-1} (Vidal et al., 2010).

The common archive period for the two reanalysis data archives is from 1 August 1958 to 31 July 2002. The period 1 August 1982–31 July 2002 is used to optimise the geopotential predictor domains except for the sensitivity test on archive length where the whole common archive is used. This is discussed later in Sect. 4.

2.1.2 Case study zones

The domain optimisation was performed for all 608 zones in the Safran dataset, but detailed sensitivity tests focused on three case study zones. All three selected zones are part of the Rhône catchment, but have different precipitation climates as shown in Fig. 2. This has implications on the spatial coherence, since different parts of the catchment receive precipitation in different meteorological situations and this may lead to different informative spatial predictor domains and therefore different analogue dates. Furthermore in Sect. 3.1 results are shown for zones located at the geographical limits of the the country. Relevance maps from these zones were used in a preliminary analysis to define the edges of the search domain. These as well as the case study zones are colored in Fig. 1.

The case study zone called *Saône* (212) is located in the Burgundy region, in the Saône river valley. The terrain is rather flat and the zone is mainly influenced by the westerlies. The precipitation is uniformly distributed over the whole year. The second zone, named *Arve* (317), is located in the upper Arve catchment near the Mont Blanc. The precipitation has a yearly cycle with a maximum in winter and a minimum in summer and early autumn. The third case study zone, named *Ardèche* (442), is located in the upper Ardèche catchment in the Cévennes area and has a precipitation maximum in October with high inter-annual variability (Vidal et al., 2010, Fig. 4). The precipitation

HESSD
10, 4015–4061, 2013

maximum in autumn results from heavy precipitation events that are frequently observed in the Cévennes region during autumn (see, e.g. Ricard et al., 2012).

2.2 Downscaling method

The downscaling method used here is an analogue approach that has already a long history of development. Duband (1981) was the first who applied the analogue method in France. Guilbaud and Obled (1998) introduced the analogue selection on gridded geopotential fields with the Teweles and Wobus shape criteria (Teweles and Wobus, 1954). Obled et al. (2002) calibrated the method for 50 French, Spanish and Italian catchments. Bontron and Obled (2005) introduced the use of reanalysis data as historical archive, the NCEP/NCAR reanalysis (Kalnay et al., 1996), instead of interpolated radiosonde data and added local humidity to the predictor variables. Ben Daoud et al. (2011a,b) introduced the temperature and the vertical velocity predictor variables. The algorithm developed by Ben Daoud et al. (2011a) is used here. The main characteristics are summarised below, for details see Ben Daoud (2010). The predictor variables, similarity criterion and the number of analogue situations selected after each step are summarised in Table 1. The algorithm performs a four-step analogue selection. The number of analogue dates retained after step 2, 3 and 4 were taken from Ben Daoud (2010). The precipitation value for day D corresponds to the precipitation accumulated between 06:00 UTC day D and 06:00 UTC day D+1.

The first step is a selection on temperature at 925 hPa at 12:00 UTC day D+1 and 600 hPa at 12:00 day D. The predictor domain is the ERA-40 grid point closest to the target location, which is reasonable as temperature can be seen as a proxy for the thermodynamical properties of the air on the local scale. A similar choice was made by Hanssen-Bauer et al. (2003). The similarity criteria is the Euclidean distance with equal weights for the two pressure levels. As shown by Timbal et al. (2008) and Hanssen-Bauer et al. (2003), including a temperature variable as a predictor is especially important in a climate change context since different temperatures may occur in a given season and the amount of water the atmosphere can hold depends on temperature.

HESSD
10, 4015–4061, 2013

The number of analogue situations selected in step one depends on the length of the archive, it is 100× number of years in the archive – for example 2000 analogue situations for a 20 yr archive as it is used for the optimisation of the predictor domains for geopotential. This approximates the four month season length used by Bontron (2004) and the 2900 days Ben Daoud (2010) used with a 30 yr archive. The four days before and after the target date are excluded to avoid the selection of days that are similar because they are close in time if like in this study the test period is equal to the archive period during optimisation.

The second step is a selection on geopotential at 1000 hPa at 12:00 UTC day D and 500 hPa at 00:00 UTC day D+1. The similarity criteria used is the Teweles and Wobus criteria S1 (Teweles and Wobus, 1954), called TWS in the following, which measures the similarity between the zonal- and meridional gradients between different points of the predictor domain and therefore measures the similarity of the shape of the fields. Guilbaud and Obled (1998) found that the TWS leads to better downscaling performance than the Euclidean distance for the geopotential predictor. This criterion has been widely used in various analogue methods (e.g. Wetterhall et al., 2005, 2007; Teutschbein et al., 2011; Horton et al., 2012a; Brigode et al., 2012) and weather type classification (e.g. Garavaglia et al., 2010). Again equal weights are given for the two pressure levels. For this step the predictor domains are optimised using the method described later in Sect. 2.5. The 170 most similar days regarding geopotential shape out of the 2000 with the most similar temperature are selected. Geopotential- or pressure fields are often used as predictors because they are well simulated by the GCMs and contain information about the atmospheric dynamics like flow strength and direction or divergence (Wilby and Wigley, 2000).

The third step is a selection on vertical velocity at 850 hPa at 06:00, 12:00 and 18:00 day D and 00:00 day D+1. The similarity criteria is Euclidean distance and the predictor domain is the nearest ERA-40 grid cell. Equal weights are given to the different times. Upward motion is necessary for the formation of clouds and precipitation. With a model resolution of 2.5° this predictor can only account for large scale upward motion due to

HESSD
10, 4015–4061, 2013

dynamical reasons and not for upward motion due to local convection or orography. Ben Daoud et al. (2011a) found some additional skill for the first two forecast days and fewer false alarms with the vertical velocity added as a predictor. The most similar 70 days out of the 170 days remaining after step two are selected.

The fourth step is a selection on humidity, more precisely the product of the total column water (TCW) and relative humidity at 850 hPa (RH) at 12:00 day D and 00:00 day D+1. This compound variable was found to be more informative than other simple indicators by Bontron (2004). The similarity criteria is Euclidean distance and the predictor domain is the nearest ERA-40 grid cell. The most similar 25 days out of the 70 days remaining after step three are selected.

The predictor variables, their pressure levels and hours and the number of analogues to select after each step were taken from Ben Daoud (2010) where they were selected for the Seine and Saône basins. It has also to be noted that identical combinations of variables, pressure levels and hours in steps 2 and 4 had also been selected by Bontron and Obled (2005) for application at various locations in south-eastern France.

2.3 Performance criterion

The skill of the downscaling method is assessed with the Continuous Ranked Probability Score (CRPS) (Brown, 1974; Matheson and Winkler, 1976). The CRPS is a probabilistic score and is widely used for the verification of probabilistic atmospheric or hydrological forecasts (see, e.g. Hagedorn et al., 2008; Demargne et al., 2010; Aspelien et al., 2011). It is defined as follows:

$$\mathrm{CRPS} = \int_{-\infty}^{\infty} \left[F(x) - H_{x_{\mathrm{obs}}^0}(x) \right]^2 dx \tag{1}$$

where $F(x)$ is the forecasted cumulative distribution function of the variable x, x_{obs}^0 the observed value and $H_{x_{\mathrm{obs}}^0}(x)$ the Heavyside function of $x - x_{\mathrm{obs}}^0$. The properties of

HESSD
10, 4015–4061, 2013

the CRPS are as described in Hersbach (2000): the CRPS is sensitive to the entire range of the parameter, no predefined classes are required, it is equal to the mean absolute error (MAE) in the case of a deterministic forecast and it can be interpreted as an integral over all possible Brier scores. In order to compare results from different zones the Continous Ranked Probability Skill Score (CRPSS) with the climatology as a reference forecast is used.

$$\mathrm{CRPSS} = 1 - \frac{\mathrm{CRPS}}{\mathrm{CRPS}_{\mathrm{climatology}}} \quad (2)$$

The $\mathrm{CRPS}_{\mathrm{climatology}}$ is calculated using precipitation data from ±60 days around the target day from different years in order to take seasonality into account.

2.4 Relevance maps

A relevance map represents the forecast skill for each grid cell of the predictor dataset. Relevance maps were used for example by Bontron (2004) and Horton et al. (2012a) to select the most predictive pressure level and time step for the geopotential predictor. Relevance maps are obtained by fixing every parameter except the location of a unitary sized spatial domain (2×2 ERA-40 grid points, 2.5° resolution) that moves across the whole map (Horton et al., 2012a). By iterating the position of this small domain, the CRPS score corresponding to every spatial unit is obtained. Relevance maps thus allow to see where the synoptic circulation information is relevant to explain observed or analysed precipitation time series. It is expected that the best predictor locations are consistent with the meteorological characteristics that are responsible for the region's weather. The predictor's best locations are therefore expected to be different for sub-catchments or stations influenced by different meteorological phenomena (Horton et al., 2012a).

Relevance maps are used in this study (1) to illustrate the different atmospheric influences for zones in different parts of the country (Sect. 3.1), (2) to compare the optimised domains with the regions of high skill in the relevance maps (Sect. 3.2.2),

HESSD
10, 4015–4061, 2013

and (3) to have an additional starting point for experiments on the sensitivity of the optimisation algorithm (Sect. 3.3.1).

2.5 Optimisation method

For the geopotential predictor a larger region may be relevant for the local precipitation and the size and location of the optimised domain may vary even for target locations close to each other. Therefore it is important to optimise the predictor domains for geopotential for each target location depending on the meteorological influences that are responsible for the precipitation.

The selected optimisation method is based on the idea of growing rectangular domains as applied by Bontron (2004) and Ben Daoud (2010). The basic version starts from a given 2 × 2 grid point domain, calculates a score, here the CRPS, and then expands the domain in 4 directions by adding one gridpoint east, west, north or south. For this 4 resulting domains the CRPS is calculated and the domain with the smallest CRPS is selected. This selected domain is used as a starting domain in the next step. This is done until the score is not improved during 4 consecutive steps or the edge of the search domain is reached. This method is very fast, but explores only a very small subset of the space of predictor domains and therefore it is likely that some relevant domains are not tested.

For this work an extended version of this method, where 5 domains are retained and expanded in each step was developed. With this method a larger number of domains is explored and the five best domains found in this procedure are returned, thus providing an indication of variability around optimal domains. In the first step there are only 4 domains and all of them are expanded in the next step. This gives 16 domains, but only 10 actually different ones, so 10 new domains are explored. From this 10 the 5 best are selected for the next step. Theoretically there are up to 20 domains (5 × 4) to explore from step 3 on, but there is some redundancy or some domains already explored in a previous step so that between 13 and 18 actually new ones were found. For the starting domain the nearest 2 × 2 grid points domain to the target zone is used.

HESSD
10, 4015–4061, 2013

Brigode et al. (2012) optimised the predictor domains for a rainfall based weather pattern classification and therefore tested domains of three different sizes for every possible location similar to the relevance map calculation. This is a complementary approach to the one used in this work since they assumed a domain size and shape and then tested where to center it. In the present work, a starting point is fixed, which defines a location that has to be included in the final domain, and then domains of different size and shapes but all containing the starting point are tested. A approach similar to the one adopted by Brigode et al. (2012) was chosen by Obled et al. (2002) for a previous version of the analogue method used here. They first tested domains of six different sizes centered over the target location and then shifted the best one to find the best location. Sauter and Venema (2011) optimised the predictor domains for an artificial neural network for all predictor variables together, allowing three dimensional and disjointed predictor domains. In contrast to our study, they did the optimisation for only one target location and even for this one location they stated that the computational costs were very high.

3 Results

In the following sections results are shown on the different regions of influence as mapped with relevance maps (Sect. 3.1), the size and location of the optimised predictor domains (Sect. 3.2), the downscaling skill of the method using the optimised domains during the optimisation period (Sect. 3.2.1) and sensitivity experiments on the choice of the starting point of the optimisation, the choice of the basic or extended optimisation method and the archive length (Sect. 3.3).

The downscaling and optimisation methods are implemented in Fortran 2003 using the NetCDF Fortran90 library (Pincus and Rew, 2011) for data input and output. The subsequent analysis and figures are done using the R software environement (R Development Core Team, 2012) with packages ncdf (Pierce, 2011), ggplot2 (Wickham, 2009), reshape2 (Wickham, 2007), RColorBrewer (Neuwirth, 2011; Harrower and

HESSD
10, 4015–4061, 2013

Brewer, 2003), sp (Pebesma and Bivand, 2005; Bivand et al., 2008), zoo (Zeileis and Grothendieck, 2005) and gridExtra (Auguie, 2012).

3.1 Different regions of influence

The relevance maps for different Safran zones located at the geographical limits of France and in the Rhône basin (cf. Fig. 1) and calculated with the 20 yr archive are compared in Fig. 3. This figure also contains the corresponding optimised domains that will be discussed later in Sect. 3.2.2. First the magnitude of the skill differs between the relevance maps for different zones. The highest skill is found for zones that are mainly exposed to the westerlies (127, 557, 317). Furthermore there is a clear difference in the spatial pattern between different zones. The zones in western-, northern- and north-eastern France (001, 074, 127, 557, 317) have their region of maximum skill located west or southwest from the zone. Their regions of high skill are larger in zonal direction than in meridional direction and are cyclonically curved. They are exposed to the westerlies and receive precipitation mainly from frontal systems. A similar shape was found by Horton et al. (2012a) for the Marécottes station in Switzerland, located close to the Arve zone (317). The zones in south-eastern France have their region of maximum skill located south or south-east from the zone (493, 596, 442, 615). Indeed, the heavy precipitation events in this region are associated with southerly or south-easterly flow (e.g. Ricard et al., 2012). Their regions of highest skill are more north-south oriented with high skill regions extending westward at the southern end and eastward and northwestward at the northern end. What all relevance maps have in common is a local minimum of skill surrounded by regions with higher skill. This is due to the use of the TWS criterion that is sensitive to the gradients of the geopotential fields and their anomalies on days with precipitation. The region of low skill corresponds to the location of a minimum in the mean geopotential anomaly fields for rainy days (not shown). The largest gradients are situated around this minimum which makes this regions more relevant using a similarity measure based on gradients.

HESSD
10, 4015–4061, 2013

Given the high seasonality with the precipitation maximum in autumn for the Ardèche case study zone (442) (cf. Fig. 2) due to specific atmospheric flow conditions, we investigated the score variations for different seasons. Seasonal relevance maps were obtained by averaging the CRPSS over different seasons instead of the whole year. In order to have enough data for each season the score was calculated for the whole 44 yr archive. Relevance maps for the Ardèche case study zone for different seasons are shown in Fig. 4. The highest skill can be found for the winter season followed by autumn. The location of the maximum of skill southeast to south-southeast from the Ardèche target zone corresponds well with the south-southeasterly flow found by Duffourg and Ducrocq (2011) for heavy precipitation events in the Cévennes region. In spring and summer the skill is lower due to convective precipitation which is more difficult to predict based only on large scale fields. This is a common feature for the three case study zones (not shown). Interestingly the shape of the region with high skill is very similar between the seasons which was not expected for the Ardèche zone due to the specific flow condition that leads to the autumn precipitation maximum in this zone (cf. Fig. 2). Further investigation could look at relevance maps for days with different precipitation thresholds, but this is beyond the scope of this paper.

3.2 Optimised predictor domains

In this section we will show results on the optimised domains. The downscaling skill measured with the CRPSS for all 608 zones in France is shown first. The near-optimum domains found for the case study zones are then presented, before looking at summary characteristics for all 608 zones in France.

3.2.1 Downscaling skill

Figure 5 shows the CRPSS over the 20 yr optimisation period for the best domains found. The CRPSS shows unsurprisingly a spatial distribution similar to the one of the mean precipitation (Vidal et al., 2010). The more precipitation a region receives the

HESSD
10, 4015–4061, 2013

higher the CRPSS. The highest skill, between 0.30 and 0.35, is found on the windward side (west side in this case) of the Alps, the Massif Central and the Vosges and along the Atlantic coast. Poorer skill, around 0.2, can be found on the lee side of mountains and around the Mediterranean coast.

Figure 6 shows the difference in skill between the best and the fifth best domain found. The differences in skill measured with the CRPSS between the best and the fifth best domain are never larger than 0.01. So the difference in skill between different optimised domains for the same zone are about one order of magnitude smaller than the differences in skill between different zones. This makes all five domains equally plausible.

3.2.2 Case study zones

As shown in Fig. 3, the optimised domains tend to include the most relevant area depicted by the relevance maps for the case study zones. They differ reasonably between different locations and inside the ensemble for a given zone. For the majority of the zones (074, 127, 493, 557, 615, 317) the aspect ratio of the optimised domains varies little inside the five domain ensemble while there are larger variations of this property for 001, 596 and 442 zone. This large differences in aspect ratio do not lead to larger differences in skill as can be seen in Fig. 6.

3.2.3 Domain characteristics at the scale of France

Figure 7a shows the mean location of the center of the optimised domains for each of the 608 zones using a 2-D colour scheme for bivariate maps introduced by Teuling et al. (2011). Here the two variables that are combined are the longitude and the latitude of the domain center. The domain centers for the best domains are mainly distributed following the location of the target zone but there are some deviations. For zones on the east side of the Massif Central the centers of the optimised domains are located clearly more east than the ones for zones on the west side of the massif. The same feature

HESSD
10, 4015–4061, 2013

can be seen at other mountain ridges, for example the Vosges mountain. Furthermore the domain centers for the zones in southeastern France are located more east than north of this area. In some regions like for example Champagne in the northeast of the country (approximate Lambert coordinates $X = 700$, $Y = 2400$) we can see that many zones have their average optimised domain center at approximately the same location. In contrast for the Cévennes and the southern Alpes regions the average domain centers differ more often between neighbouring zones.

Figure 7b shows the maximum difference in domain center location between two domains in the five best domain ensemble. For the majority of the zones the domain center location is a very stable property especially in latitude direction where differences of more than two degrees are rare. Zones with larger differences, up to eight degrees in longitude, are located in the southeastern part of the country at the slopes of the Alpes and the Massif Central.

Figure 8a shows the mean size in degrees longitude and latitude of the optimised domains for each zone. Again the 2-D colour scheme is used with the mean domain length in zonal direction and the mean domain length in meridional direction being the two variables. Small optimised domains (green colour) can be found in Brittany (150, 2400), in Champagne (750, 2500), Lorraine (850, 2450), Poitou–Charentes (300, 2200) and in some parts of Normandy (300, 2500). Optimised domains with small extent in longitude direction but somewhat larger extent in latitude direction (blue colour) can be found along the Mediterranean coast and in the northernmost part of the country. Domains with small extent in the latitude direction and larger extent in the longitude direction (yellow) form a east-west oriented band in the middle of the country (around 2250 km Y Lambert). Medium sized domains (gray, brown) are found north of this band (500–900, 2350), in the south-west of the country and on the west side of Corsica (1150, 1700). The largest domains (purple, red, dark blue) tend to be situated in the south-eastern part of France, except near the coast. The most prominent feature in this map is the area in the middle where the optimised domains are very small in the meridional direction, while being reasonably stretched zonally.

HESSD
10, 4015–4061, 2013

Figure 8b shows the ratio of domain size range in the five domain ensemble, defined as follows:

$$\text{ratio} = \frac{\max(X) - \min(X)}{\text{mean}(X)} \quad (3)$$

where X is the extent of the domains in degrees longitude or latitude respectively. A size ratio of 0 means that all five domains have equal extent. A size ratio of 1 means that the difference in extent between the largest and the smallest domain is equal to the mean extent. On average the size ratio is larger in longitude direction than in latitude direction. The figure is quite patchy with individual zones showing large ratios in one or both dimensions. In the north of the country and along the Mediterranean coast these individual zones have large ratios in longitude or both dimensions. The zones 001 and 596 shown in Fig. 3 are examples of such zones. The zones with the largest domain size range in the latitude direction are situated in the southern half of the country, except near the Mediterranean coast.

3.3 Sensitivity experiments

For the domain optimisation, choices were made concerning the choice of the algorithm, the starting point and the archive length. In this section we take a detailed look at the impact of these choices on the optimised domains for the three case study zones by comparing with results for alternative choices.

3.3.1 Starting domain for optimisation

The optimisation of predictor domains is often started from domains centered on the target location (e.g. Obled et al., 2002) or nearest grid cell (e.g. Sauter and Venema, 2011), but for the growing rectangular domains (Bontron, 2004; Ben Daoud, 2010) started at the most relevant elementary domain.

The domain optimisation algorithm used in this work requires a predefined elementary domain to start the optimisation, that has to be included in the final predictor

HESSD
10, 4015–4061, 2013

domain. One reasonable assumption is that the best predictor domain will comprise the large scale grid cell closest to the target location as it is done here. Another possibility is to start at the most relevant elementary domain as obtained through a relevance map to make sure that the most relevant location is included in the final predictor domain. The drawback of the second approach is that the computational costs for the relevance maps are high if performed for over 600 target locations. Roughly 2.8 million CRPS calculations per zone are for example needed for a 40 × 60 degree sized relevance map with a 20 yr archive. Therefore the relevance maps were computed only for the case study zones and for these zones the optimised domains obtained with the two different starting domains are compared.

The first line of Fig. 9 shows the five best domains found with the optimisation procedure starting at the nearest elementary domain, with a 20 yr archive. In the second line the same procedure is used, but the optimisation was started from the most relevant elementary domain as found with the relevance map. Comparing them we can see that for the Arve zone and the Ardèche zone exactly the same five domains are found even if the two starting domains are different. For the Saône zone, five different domains are found, with lower meridional extent and systematically higher zonal extent when starting from the most relevant elementary domain.

Doing the same experiment but with the basic algorithm, the same best domain (shown in Fig. 10, second line) is found with the different starting domains using the 20 yr archive. On one hand, it shows that indeed better domains can be found if more possible domains are explored through the extended algorithm and on the other hand it highlights some limitations of starting the optimisation algorithm from the nearest grid cell. A possible "low-cost" improvement could be to calculate scores for example the four nearest elementary domains and then start the optimisation from the best out of them.

HESSD
10, 4015–4061, 2013

3.3.2 Optimisation method

Results obtained with the basic and the extended optimisation algorithm are compared for the case study zones. Figure 10 shows the optimised domain found with the extended algorithm (first row) and the ones found with the basic algorithm. For the Arve zone the best domain is the same for the two algorithms. For the Saône zone and the Ardèche zone the domain found with the basic algorithm is the second best found with the extended version. This shows that for some zones it is possible to find better domains with the extended algorithm. Furthermore the five domains give an indication of variability between equally skillful different domains for a zone since it was shown in Sect. 3.2.1 that the skill difference between the five domains is very small.

3.3.3 Archive length

The optimised predictor domains obtained with a 20 yr archive (1 August 1982–31 July 2002) are here compared with the optimised predictor domains obtained with a 44 yr archive (1 August 1958–31 July 2002). Figure 11 shows the optimised domains found with the 20 yr archive (first row) and 44 yr archive (second row). There are slightly different optimised domains found for the different archive lengths. For the Arve zone (second column) the differences between the best domains found with the two archive lengths are small. The best domain found with the 20 yr archive is one grid cell larger in the west than the one found with the 44 yr archive and was found 5th best with the 44 yr archive. All top 5 domains found have the same extent in meridional direction. For the Saône zone (first column) the domains found with different archive lengths differ, but the second best domains found are the same and the best domain found with the 44 yr archive is the same as the 5th best found with the 20 yr archive. For the upper Ardèche zone five completely different domains are found with the different archive lengths. This is probably related to the high inter-annual variability in the target region (Vidal et al., 2010).

HESSD
10, 4015–4061, 2013

Additionally, the relevance maps obtained with different archive lengths show the same structure and the same location of maximum values but the absolute values are slightly higher with the longer archive. On relevance maps obtained with a 10 yr archive (not shown) the same overall structure is still visible but with a decrease in CRPSS of approximately one-third.

4 Discussion

4.1 Choice of the archive period

For successful statistical downscaling it is necessary to have long data sets of predictors and predictands for building and validating the model (Timbal and McAvaney, 2001). The archive length and optimisation period chosen for statistical downscaling development depends strongly on the data that are available and the validation strategy. Bontron (2004) and Ben Daoud (2010) left only five years of their archive for validation. Ben Daoud (2010) for example excluded the years 1978, 1983, 1988, 1993 and 1998 from the 1972–2002 optimisation period. The specific years were chosen to resemble the 1972–2002 climate as closely as possible. This approach was designed to validate the method for forecast purposes in the same climate. The advantage of keeping only a small part of the data for validation is a longer archive. Timbal et al. (2003) found that using more than 20 yr of the reanalysis archive does not further reduce the error in the reconstructed time series as long as the more recent part of the data is used, indicating that data quality plays an important roll too.

The sensitivity of the optimised domains on the archive was examined for three case study zones revealing varying degree of sensitivity for the different zones. For the Ardèche zone five completely different domains are for example found with the different archive lengths. When the downscaling method is applied on an independent validation period, it would be interesting to see if the skill degrades more than for the other zones.

HESSD
10, 4015–4061, 2013

4.2 Optimisation starting point

The starting point for optimisation was chosen to be the nearest elementary domain to the target zone. The optimisation method used requires that this elementary domain is included in the final domains. The break line at 47.5° N that can be seen in Fig. 8a is a result of this choice. Our Saône case study zone happens to be situated north of this break line and the experiment with an alternative starting point, more southwest in this case, showed that the optimised domains differ for this case study zone while they rest the same for the other case study zones. The domains found starting at the most relevant elementary domain achieve a 3 % larger CRPSS. The domains found starting the optimisation from the most relevant elementary domain are indeed very similar to those found for zones south of the Saône case study zone (not shown).

5 Conclusions

5.1 On the assumption of a common predictor domain

This work addressed the validity of the assumption of a common predictor domain for different regions of France for statistical downscaling of precipitation. This assumption has been indeed made implicitly by all previous studies over France, e.g. Timbal et al. (2003) for western and southern France separately and Boé and Terray (2008) for the whole of France. Results from the optimisation of geopotential predictor domains showed a large diversity of near-optimum domains for the set of 608 climatically homogeneous zones covering France, and therefore suggest that this assumption is questionable, at least when one seeks to obtain the most skillful method for each individual zone. However, relatively large zones have been found to share similar near-optimum predictor domains and making this assumption within each of them may lead to limited loss of skill compared to domains optimised for individual locations. Conversely, large river basins like the Rhône basin include zones with very diverse influence as

HESSD
10, 4015–4061, 2013

exemplified by the three case study zones located in the Saône, upper Arve and upper Ardèche catchments (see Fig. 3).

The most widely used statistical downscaling method in France for climate change impact studies is currently *dsclim* (Pagé et al., 2008; Pagé and Terray, 2010) in which a common domain for the mean sea level pressure predictor is defined for all locations in France. This method has been initially developed for the Seine basin by Boé et al. (2006, 2007) where the unique predictor domain assumption appears reasonably valid in light of the results presented in Figs. 7 and 8. It has been later extended to the whole of France by Boé and Terray (2008), then used in many subsequent climate change impact studies on hydrology (see, e.g. Boé et al., 2009; Vidal et al., 2012), and downscaled products are now disseminated through a national climate service platform built in the DRIAS project (Lémond et al., 2011). The present work strongly suggests that the performance of this method is far from optimal for individual locations in France as a consequence of the assumption of a common predictor domain. It provides some explanation to identified biases (Boé, 2007) and weak correlations (Boé and Terray, 2008) in downscaled precipitation outputs for regions around the Mediterranean coast. Indeed, as shown in Figs. 7 and 8, the optimum geopotential predictor domains for these regions are quite different from the rest of the country.

5.2 Summary of findings

These conclusions first built on relevance maps for several case study zones which highlight regions of influence for geopotential. The highest skill values was found for zones along the Atlantic coast and in the Alps. Zones in western- northern- and north-eastern France have their region of maximum skill located west or southwest from the zone while for zones in south-eastern France it is located south or south-east from the zone. Furthermore these two groups differ in the shape of their high skill region.

The domains resulting from an optimisation with an extended version of the growing rectangular domain algorithm include the most relevant area depicted by the relevance maps for all case study zones. The domains differ moderately between different

HESSD
10, 4015–4061, 2013

locations and inside the ensemble for a given zone. The centers of the optimised domains are mainly distributed following the geographical location of the target zone but with clear differences between eastern- and western slopes of mountain ridges. The domain centers for zones in south-eastern France are located more east than north of this area. The domain center location is a stable property in the five domain ensemble except for isolated zones at the slopes of the Alps and the Massif Central. The domain sizes vary considerably between the zones with ensemble mean zonal extents between 6.5° and 28.5° and meridional extents between 5° and 15.5°. Small domains are mainly located in northern and western France, domains with small zonal and larger meridional extent in the very north and along the Mediterranean coast. Domains with small meridional and larger zonal extent form a east-west oriented band in the middle of the country. Medium sized domains are found in the south-west and on Corsica and the largest ones in south-eastern France. In some regions like Brittany we found a larger region with the same optimised domain while especially in the Rhône catchment we found high variability in the location and even more in the size of the optimised predictor domains. For the majority of the zones the aspect ratio of their five domains is rather similar, but for some zones equally skillful domains with very different aspect ratios are found.

The downscaling skill measured with the CRPSS during the optimisation period has a spatial distribution similar to the one of the mean precipitation. The differences in skill between the best and the fifth best domain found is one order of magnitude smaller than the differences in skill between different zones which makes all five domains equally plausible.

A sensitivity on the starting point for the optimisation was found for the Saône case study zone. Indeed, it belongs to a group of zones situated north of a region where the zones have optimised domains with a small meridional extent and situated rather south of the zone. The more northern group would benefit from domains similar to the ones for the zones south of them, but this domains are not found due to the mandatory inclusion of the nearest elementary domain that is more north. Their slightly larger domains

HESSD
10, 4015–4061, 2013

lead to a break-line in the mean domain size graph. The sensitivity on the optimisation algorithm was found to be low as the basic algorithm found either the best or the second best domain found by the extend version of the algorithm. The optimised domains are only sensitive to the archive length for zones with a high interannual variability like the Ardèche one.

5.3 Towards predictand areas with homogeneous predictors

The spatial coherence of the downscaled precipitation is often taken as given when using the analogue method, but this is only true if the same analogue dates are found for the whole target region, which is not guarantied if different subtarget regions are using different predictor domains. On the other hand, if the target region is large, like a large river basin, a common predictor domain is likely to be suboptimal on the local scale as the best domains differ for the subcatchments as shown in this study for example for the Rhône catchment.

Despite the simplicity of the concept, the analogue method has a large number of parameters: the predictor variables and their spatial and temporal domains, the similarity criteria and the number of analogues. A global optimisation of all these parameters together is desirable but involves high computational costs. Sauter and Venema (2011) and Horton et al. (2012b) did a global optimisation of spatial predictor domains for a small number of predictand locations. In this work the optimisation was restricted to the horizontal domains of the geopotential predictor but was done for a large number of predictand zones.

Using individual predictor domains for each zone will in general result in different analogue dates. With different analogue dates the analogue method looses the spatial coherence it has if the same parameters were used for all predictand locations. Therefore it will be beneficial to group zones together that can use the same parameters, i.e. the same geopotential predictor domain. The presented analysis will help to this end. The idea is to group zones by equal domains in the five domain ensemble, as equal optimised predictor domains reflect proximity and similar flow exposure. To this end for

HESSD
10, 4015–4061, 2013

each zone one predictor domain from the five domain ensemble has to be selected such that contiguous areas with the same predictor domain are formed. The smooth distribution of the domain center locations together with their rather small range should facilitate this. The domain size has a higher spatial variability that could hamper the attempt of aggregating zones by same domain, but this goes along with a larger range that may compensate it to a certain degree.

Acknowledgements. The authors would like to thank Météo-France for providing access to both the Safran and ERA-40 databases.

References

Aspelien, T., Iversen, T., Bremnes, J. B., and Frogner, I.-L.: Short-range probabilistic forecasts from the Norwegian limited-area EPS: long-term validation and a polar low study, Tellus A, 63, 564–584, doi:10.1111/j.1600-0870.2010.00502.x, 2011. 4025

Auffray, A., Clavel, A., Jourdain, S., Ben Daoud, A., Sauquet, E., Lang, M., Obled, C., Panthou, G., Gautheron, A., Gottardi, F., and Garçon, R.: Reconstructing the hydrometeorological scenario of the 1859 flood of the Isère river, Houille Blanche, 44–50, doi:10.1051/lhb/2011005, 2011. 4020

Auguie, B.: gridExtra: functions in Grid graphics, available at: http://CRAN.R-project.org/package=gridExtra, last access: 27 March 2013, r package version 0.9.1, 2012. 4029

Beaulant, A.-L., Joly, B., Nuissier, O., Somot, S., Ducrocq, V., Joly, A., Sevault, F., Deque, M., and Ricard, D.: Statistico-dynamical downscaling for Mediterranean heavy precipitation, Q. J. Roy. Meteorol. Soc., 137, 736–748, doi:10.1002/qj.796, 2011. 4017

Bellone, E., Hughes, J. P., and Guttorp, P.: A hidden Markov model for downscaling synoptic atmospheric patterns to precipitation amounts, Clim. Res., 15, 1–12, 2000. 4018

Ben Daoud, A.: Améliorations et développements d'une méthode de prévision probabiliste des pluies par analogie. Application à la prévision hydrologique sur les grands bassins fluviaux de la Saône et de la Seine, Thèse de doctorat, Université Joseph Fourier, Grenoble, 2010. 4019, 4023, 4024, 4025, 4027, 4033, 4036

HESSD

10, 4015–4061, 2013

Ben Daoud, A., Sauquet, E., Lang, M., Obled, C., and Bontron, G.: Precipitation forecasting through an analog sorting technique: state of the art and further investigations, Houille Blanche, 6, 60–65, doi:10.1051/lhb/2009079, 2009. 4021

Ben Daoud, A., Sauquet, E., Lang, M., Bontron, G., and Obled, C.: Precipitation forecasting through an analog sorting technique: a comparative study, Adv. Geosci., 29, 103–107, 1doi:0.5194/adgeo-29-103-2011, 2011a. 4023, 4025

Ben Daoud, A., Sauquet, E., Lang, M., and Ramos, M.-H.: Can we extend flood forecasting lead-time by optimising precipitation forecasting based on analogs? Application to the Seine river basin, Houille Blanche, 37–43, doi:10.1051/lhb/2011004, 2011b. 4020, 4023

Bivand, R. S., Pebesma, E. J., and Gomez-Rubio, V.: Applied spatial data analysis with R, available at: http://www.asdar-book.org/, Springer, NY, 2008. 4029

Boé, J.: Changement global et cycle hydrologique: une étude de régionalisation sur la France, Thèse de doctorat, available at: http://thesesups.ups-tlse.fr/227/, Université Toulouse 3, 2007. 4038

Boé, J. and Terray, L.: A weather-type approach to analyzing winter precipitation in France: twentieth-century trends and the role of anthropogenic forcing, J. Climate, 21, 3118–3133, doi:10.1175/2007JCLI1796.1, 2008. 4017, 4019, 4020, 4037, 4038

Boé, J., Terray, L., Habets, F., and Martin, E.: A simple statistical-dynamical downscaling scheme based on weather types and conditional resampling, J. Geophys. Res., 111, D23106, doi:10.1029/2005JD006889, 2006. 4017, 4018, 4038

Boé, J., Terray, L., Habets, F., and Martin, E.: Statistical and dynamical downscaling of the Seine basin climate for hydro-meteorological studies, Int. J. Climatol., 27, 1643–1655, doi:10.1002/joc.1602, 2007. 4038

Boé, J., Terray, L., Martin, E., and Habets, F.: Projected changes in components of the hydrological cycle in French river basins during the 21st century, Water Resour. Res., 45, W08426, doi:10.1029/2008WR007437, 2009. 4017, 4038

Bontron, G.: Prévision quantitative des précipitations: adaptation probabiliste par recherche danalogues. Utilisation des réanalyses NCEP/NCAR et application aux précipitations du Sud-Est de la France, Thèse de doctorat, Institut National Polytechnique de Grenoble, 2004. 4019, 4024, 4025, 4026, 4027, 4033, 4036

Bontron, G. and Obled, C.: L'adaptation probabiliste des prévisions météorologiques pour la prévision hydrologique, Houille Blanche, 23–28, doi:10.1051/lhb:200501002, 2005. 4023, 4025

HESSD
10, 4015–4061, 2013

Brigode, P., Bernardara, P., Gailhard, J., and Ribstein, P.: Optimization of the geopotential heights informatio used in a rainfall based weather patterns classification over Austria, Int. J. Climatol., doi:10.1002/joc.3535, in press, 2012. 4024, 4027, 4028

Brown, T. A.: Admissible Scoring Systems for Continuous Distributions, The Rand Paper Series, P-5235, The Rand Corporation, Santa Monica, California, 1974. 4025

Carreau, J. and Vrac, M.: Stochastic downscaling of precipitation with neural network conditional mixture models, Water Resour. Res., 47, W10502, doi:10.1029/2010WR010128, 2011. 4017

Chandler, R. E.: On the use of generalized linear models for interpreting climate variability, Environmetrics, 16, 699–715, doi:10.1002/env.731, 2002. 4018

Chen, J., Brissette, F. P., and Leconte, R.: A daily stochastic weather generator for preserving low-frequency of climate variability, J. Hydrol., 388, 480–490, doi:10.1016/j.jhydrol.2010.05.032, 2010. 4018

Dee, D. P., Uppala, S. M., Simmons, A. J., Berrisford, P., Poli, P., Kobayashi, S., Andrae, U., Balmaseda, M. A., Balsamo, G., Bauer, P., Bechtold, P., Beljaars, A. C. M., van de Berg, L., Bidlot, J., Bormann, N., Delsol, C., Dragani, R., Fuentes, M., Geer, A. J., Haimberger, L., Healy, S. B., Hersbach, H., Hólm, E. V., Isaksen, L., Kållberg, P., Köhler, M., Matricardi, M., McNally, A. P., Monge-Sanz, B. M., Morcrette, J.-J., Park, B.-K., Peubey, C., de Rosnay, P., Tavolato, C., Thépaut, J.-N., and Vitart, F.: The ERA-Interim reanalysis: configuration and performance of the data assimilation system, Q. J. Roy. Meteorol. Soc., 137, 553–597, doi:10.1002/qj.828, 2011. 4021

Demargne, J., Brown, J., Liu, Y., Seo, D.-J., Wu, L., Toth, Z., and Zhu, Y.: Diagnostic verification of hydrometeorological and hydrologic ensembles, Atmos. Sci. Lett., 11, 114–122, doi:10.1002/asl.261, 2010. 4025

Duband, D.: Prévision spatiale des hauteurs de précipitations journalières, Houille Blanche, 7–8, 497–512, doi:10.1051/lhb/1981046, 1981. 4023

Duffourg, F. and Ducrocq, V.: Origin of the moisture feeding the Heavy Precipitating Systems over Southeastern France, Nat. Hazards Earth Syst. Sci., 11, 1163–1178, doi:10.5194/nhess-11-1163-2011, 2011. 4030

Friederichs, P. and Hense, A.: Statistical downscaling of extreme precipitation events using censored quantile regression, Mon. Weather Rev., 135, 2365–2378, doi:10.1175/MWR3403.1, 2007. 4018

HESSD
10, 4015–4061, 2013

Garavaglia, F., Gailhard, J., Paquet, E., Lang, M., Garçon, R., and Bernardara, P.: Introducing a rainfall compound distribution model based on weather patterns sub-sampling, Hydrol. Earth Syst. Sci., 14, 951–964, doi:10.5194/hess-14-951-2010, 2010. 4024

Guilbaud, S. and Obled, C.: Prévision quantitative des précipitations journalières par une technique de recherche de journées antérieures analogues: optimisation du critère d'analogie (Daily quantitative precipitation forecast by an analogue technique: optimisation of the analogy criterion, in French), CR ACAD Sci. II A, 327, 181–188, doi:10.1016/S1251-8050(98)80006-2, 1998. 4023, 4024

Gutiérrez, J. M., San-Martín, D., Brands, S., Manzanas, R., and Herrera, S.: Reassessing statistical downscaling techniques for their robust application under climate change conditions, J. Climate, 26, 171–188, doi:10.1175/JCLI-D-11-00687.1, 2013. 4019

Hagedorn, R., Hamill, T. M., and Whitaker, J. S.: Probabilistic forecast calibration using ECMWF and GFS ensemble reforecasts, Part I: Two-meter temperatures, Mon. Weather Rev., 136, 2608–2619, doi:10.1175/2007MWR2410.1, 2008. 4025

Hamill, T. M. and Whitaker, J. S.: Probabilistic quantitative precipitation forecasts based on reforecast analogs: theory and application, Mon. Weather Rev., 134, 3209–3229, doi:10.1175/MWR3237.1, 2006. 4018

Hanssen-Bauer, I., Førland, E. J., Haugen, J. E., and Tveito, O. E.: Temperature and precipitation scenarios for Norway: comparison of results from dynamical and empirical downscaling, Clim. Res., 25, 15–27, doi:10.3354/cr025015, 2003. 4023

Harrower, M. and Brewer, C. A.: ColorBrewer.org: an online tool for selecting colour schemes for maps, Cartogr. J., 40, 27–37, doi:10.1179/000870403235002042, 2003. 4028

Hersbach, H.: Decomposition of the continuous ranked probability score for ensemble prediction systems, Weather Forecast., 15, 559–570, 2000. 4026

Hertig, E., Paxian, A., Vogt, G., Seubert, S., Paeth, H., and Jacobeit, J.: Statistical and dynamical downscaling assessments of precipitation extremes in the Mediterranean area, Meteorol. Z., 21, 61–77, doi:10.1127/0941-2948/2012/0271, 2012. 4018

Horton, P., Jaboyedoff, M., Metzger, R., Obled, C., and Marty, R.: Spatial relationship between the atmospheric circulation and the precipitation measured in the western Swiss Alps by means of the analogue method, Nat. Hazards Earth Syst. Sci., 12, 777–784, doi:10.5194/nhess-12-777-2012, 2012a. 4018, 4024, 4026, 4029

HESSD
10, 4015–4061, 2013

Horton, P., Jaboyedoff, M., and Obled, C.: Calibration of the analogue method for precipitation forecasting by means of genetic algorithms, Geophys. Res. Abstr., 14, EGU2012–2478–2, 2012b. 4020, 4040

Ibarra-Berastegi, G., Saénz, J., Ezcurra, A., Elías, A., Diaz Argandoña, J., and Errasti, I.: Downscaling of surface moisture flux and precipitation in the Ebro Valley (Spain) using analogues and analogues followed by random forests and multiple linear regression, Hydrol. Earth Syst. Sci., 15, 1895–1907, doi:10.5194/hess-15-1895-2011, 2011. 4018

Kallache, M., Vrac, M., Naveau, P., and Michelangeli, P.-A.: Nonstationary probabilistic downscaling of extreme precipitation, J. Geophys. Res., 116, D05113, doi:10.1029/2010JD014892, 2011. 4017

Kalnay, E., Kanamitsu, M., Kistler, R., W., C., Deaven, D., Gandin, L., Iredell, M., Saha, S., White, G., Woollen, J., Zhu, Y., Chelliah, M., Ebisuzaki, W., Higgins, W., Janoviak, J., Mo, K. C., Ropelewski, C., Wang, J., Leetmaa, A., Reynolds, R., Jenne, R., and Joseph, D.: The NCEP/NCAR 40-year Reanalysis Project, B. Am. Meteorol. Soc., 77, 437–471, doi:10.1175/1520-0477(1996)077<0437:TNYRP>2.0.CO;2, 1996. 4021, 4023

Lavaysse, C., Vrac, M., Drobinski, P., Lengaigne, M., and Vischel, T.: Statistical downscaling of the French Mediterranean climate: assessment for present and projection in an anthropogenic scenario, Nat. Hazards Earth Syst. Sci., 12, 651–670, doi:10.5194/nhess-12-651-2012, 2012. 4017, 4018

Lémond, J., Dandin, P., Planton, S., Vautard, R., Pagé, C., Déqué, M., Franchistéguy, L., Geindre, S., Kerdoncuff, M., Li, L., Moisselin, J.-M., Noël, T., and Tourre, Y. M.: DRIAS: a step toward climate services in France, Adv. Sci. Res., 6, 179–186, doi:10.5194/asr-6-179-2011, 2011. 4038

Liu, X. and Coulibaly, P.: Downscaling ensemble weather predictions for improved week-2 hydrologic forecasting, J. Hydrometeorol., 12, 1564–1580, doi:10.1175/2011JHM1366.1, 2011. 4018

Lorenz, E. N.: Atmospheric predictability as revealed by naturally occurring analogues, J. Atmos. Sci., 26, 636–646, doi:10.1175/1520-0469(1969)26<636:APARBN>2.0.CO;2, 1969. 4018

Maraun, D., Wetterhall, F., Ireson, A. M., Chandler, R. E., Kendon, E. J., Widmann, M., Brienen, S., Rust, H. W., Sauter, T., Themessl, M., Venema, V. K. C., Chun, K. P., Goodess, C. M., Jones, R. G., Onof, C., Vrac, M., and Thiele-Eich, I.: Precipitation downscaling

HESSD
10, 4015–4061, 2013

under climate change. Recent developments to bridge the gap between dynamical models and the end user, Rev. Geophys., 48, RG3003, doi:10.1029/2009RG000314, 2010. 4018
Martin, E., Timbal, B., and Brun, E.: Downscaling of general circulation model outputs: simulation of the snow climatology of the French Alps and sensitivity to climate change, Clim. Dynam., 13, 45–56, doi:10.1007/s003820050152, 1997. 4017
Marty, R., Zin, I., and Obled, C.: On adapting PQPFs to fit hydrological needs: the case of flash flood forecasting, Atmos. Sci. Lett., 9, 73–79, 2008. 4018
Marty, R., Zin, I., Obled, C., Bontron, G., and Djerboua, A.: Toward real-time daily PQPf by an analog sorting approach: application to flash-flood catchments, J. Appl. Meteorol. Clim., 51, 505–520, doi:10.1175/JAMC-D-11-011.1, 2012. 4018
Marty, R., Zin, I., and Obled, C.: Sensitivity of hydrological ensemble forecasts to different sources and temporal resolutions of probabilistic quantitative precipitation forecasts: flash flood case studies in the Cévennes-Vivarais region (Southern France), Hydrol. Process., 27, 33–44, doi:10.1002/hyp.9543, 2013. 4018
Matheson, J. E. and Winkler, R. L.: Scoring rules for continuous probability distributions, Manage. Sci., 22, 1087–1095, 1976. 4025
Muluye, G. Y.: Deriving meteorological variables from numerical weather prediction model output: a nearest neighbor approach, Water Resour. Res., 47, W07509, doi:10.1029/2010WR009750, 2011. 4018
Nam, D. H., Udo, K., and Mano, A.: Downscaling global weather forecast outputs using ANN for flood prediction, J. Appl. Math., 2011, 246286, doi:10.1155/2011/246286, 2011. 4018
Neuwirth, E.: RColorBrewer: ColorBrewer palettes, available at: http://CRAN.R-project.org/package=RColorBrewer (last access: 27 March 2013), 2011. 4028
Nuissier, O., Joly, B., Joly, A., Ducrocq, V., and Arbogast, P.: A statistical downscaling to identify the large-scale circulation patterns associated with heavy precipitation events over southern France, Q. J. Roy. Meteorol. Soc., 137, 1812–1827, doi:10.1002/qj.866, 2011. 4017
Obled, C., Bontron, G., and Garçon, R.: Quantitative precipitation forecasts: a statistical adaptation of model outputs through an analogues sorting approach, Atmos. Res., 63, 303–324, doi:10.1016/S0169-8095(02)00038-8, 2002. 4023, 4028, 4033
Pagé, C. and Terray, L.: Nouvelles projections climatiques à échelle fine sur la France pour le 21ème siècle: les scénarii SCRATCH2010, Technical Report TR/CMGC/10/58, CERFACS, Toulouse Cedex, France, 2010. 4038

HESSD
10, 4015–4061, 2013

Pagé, C., Terray, L., and Boé, J.: Projections climatiques à échelle fine sur la France pour le 21ème siècle: les scénarii SCRATCH08, Technical note, Climate Modelling and Global Change TR/CMGC/08/64, CERFACS, Toulouse, France, 2008. 4038

Pebesma, E. and Bivand, R.: Classes and methods for spatial data in R, r news 5 (2) Edn., available at: http://cran.r-project.org/doc/Rnews/ (last access: 27 March 2013), 2005. 4029

Pierce, D.: ncdf: Interface to Unidata netCDF data files, available at: http://CRAN.R-project.org/package=ncdf, last access: 27 March 2013, r package version 1.6.6, 2011. 4028

Pincus, R. and Rew, R.: NetCDF Fortran 90 Guide, netcdf 4.1.3 Edn., UCAR Unidata, Boulder, Colorado, 2011. 4028

Quintana-Seguí, P., Le Moigne, P., Durand, Y., Martin, E., Habets, F., Baillon, M., Canellas, C., Franchistéguy, L., and Morel, S.: Analysis of near-surface atmospheric variables: validation of the SAFRAN analysis over France, J. Appl. Meteorol. Clim., 47, 92–107, doi:10.1175/2007JAMC1636.1, 2008. 4021

Quintana-Seguí, P., Ribes, A., Martin, E., Habets, F., and Boé, J.: Comparison of three downscaling methods in simulating the impact of climate change on the hydrology of Mediterranean basins, J. Hydrol., 383, 111–124, doi:10.1016/j.jhydrol.2009.09.050, 2010. 4017

Quintana-Seguí, P., Habets, F., and Martin, E.: Comparison of past and future Mediterranean high and low extremes of precipitation and river flow projected using different statistical downscaling methods, Nat. Hazards Earth Syst. Sci., 11, 1411–1432, doi:10.5194/nhess-11-1411-2011, 2011. 4017

R Development Core Team: R: A Language and Environment for Statistical Computing, available at: http://www.R-project.org/, R Foundation for Statistical Computing, Vienna, Austria, 2012. 4028

Raje, D. and Mujumdar, P. P.: A comparison of three methods for downscaling daily precipitation in the Punjab region, Hydrol. Process., 25, 3575–3589, doi:10.1002/hyp.8083, 2011. 4018

Ricard, D., Ducrocq, V., and Auger, L.: A climatology of the mesoscale environment associated with heavily precipitating events over a Northwestern Mediterranean area, J. Appl. Meteorol. Clim., 51, 468–488, doi:10.1175/JAMC-D-11-017.1, 2012. 4023, 4029

Sauter, T. and Venema, V.: Natural three-dimensional predictor domains for statistical precipitation downscaling, J. Climate, 24, 6132–6145, doi:10.1175/2011JCLI4155.1, 2011. 4020, 4028, 4033, 4040

Teuling, A. J., Stöckli, R., and Seneviratne, S. I.: Bivariate colour maps for visualizing climate data, Int. J. Climatol., 31, 1408–1412, doi:10.1002/joc.2153, 2011. 4031

HESSD
10, 4015–4061, 2013

Teutschbein, C., Wetterhall, F., and Seibert, J.: Evaluation of different downscaling techniques for hydrological climate-change impact studies at the catchment scale, Clim. Dynam., 37, 2087–2105, doi:10.1007/s00382-010-0979-8, 2011. 4024

Teweles, S. and Wobus, H. B.: Verification of prognostic charts, B. Am. Meteorol. Soc., 35, 455–463, 1954. 4023, 4024, 4050

Themeßl, M. J., Gobiet, A., and Leuprecht, A.: Empirical-statistical downscaling and error correction of daily precipitation from regional climate models, Int. J. Climatol., 31, 1530–1544, doi:10.1002/joc.2168, 2011. 4018

Timbal, B. and McAvaney, B. J.: An analogue-based method to downscale surface air temperature: application for Australia, Clim. Dynam., 17, 947–963, doi:10.1007/s003820100156, 2001. 4018, 4019, 4036

Timbal, B., Dufour, A., and McAvaney, B.: An estimate of future climate change for western France using a statistical downscaling technique, Clim. Dynam., 20, 807–823, doi:10.1007/s00382-002-0298-9, 2003. 4017, 4018, 4019, 4020, 4036, 4037

Timbal, B., Hope, P., and Charles, S.: Evaluating the consistency between statistically downscaled and global dynamical model climate change projections, J. Climate, 21, 6052–6059, doi:10.1175/2008JCLI2379.1, 2008. 4023

Turco, M., Quintana Seguí, P., Llasat, M. C., Herrera, S., and Gutiérrez, J. M.: Testing MOS precipitation downscaling for ENSEMBLES regional climate models over Spain, J. Geophys. Res., 116, D18109, doi:10.1029/2011JD016166, 2011. 4018

Uppala, S. M., Kållberg, P. W., Simmons, A. J., Andrae, U., Da Costa Bechtold, V., Fiorino, M., Gibson, J. K., Haseler, J., Hernandez, A., Kelly, G. A., Li, X., Onogi, K., Saarinen, S., Sokka, N., Allan, R. P., Andersson, E., Arpe, K., Balmaseda, M. A., Beljaars, A. C. M., Van De Berg, L., Bidlot, J., Bormann, N., Caires, S., Chevallier, F., Dethof, A., Dragosavac, M., Fisher, M., Fuentes, M., Hagemann, S., Hólm, E., Hoskins, B. J., Isaksen, L., Janssen, P. A. E. M., Jenne, R., Mcnally, A. P., Mahfouf, J.-F., Morcrette, J.-J., Rayner, N. A., Saunders, R. W., Simon, P., Sterl, A., Trenberth, K. E., Untch, A., Vasiljevic, D., Viterbo, P., and Woollen, J.: The ERA-40 re-analysis, Q. J. Roy. Meteorol. Soc., 131, 2961–3012, doi:10.1256/qj.04.176, 2005. 4021

Vidal, J.-P. and Wade, S. D.: A framework for developing high-resolution multi-model climate projections: 21st century scenarios for the UK, Int. J. Climatol., 28, 843–858, doi:10.1002/joc.1593, 2008. 4018

HESSD
10, 4015–4061, 2013

Vidal, J.-P., Martin, E., Franchistéguy, L., Baillon, M., and Soubeyroux, J.-M.: A 50-year high-resolution atmospheric reanalysis over France with the Safran system, Int. J. Climatol., 30, 1627–1644, doi:10.1002/joc.2003, 2010. 4021, 4022, 4030, 4035

Vidal, J.-P., Martin, E., Kitova, N., Najac, J., and Soubeyroux, J.-M.: Evolution of spatio-temporal drought characteristics: validation, projections and effect of adaptation scenarios, Hydrol. Earth Syst. Sci., 16, 2935–2955, doi:10.5194/hess-16-2935-2012, 2012. 4038

Voisin, N., Schaake, J. C., and Lettenmaier, D. P.: Calibration and downscaling methods for quantitative ensemble precipitation forecasts, Weather Forecast., 25, 1603–1627, doi:10.1175/2010WAF2222367.1, 2010. 4018

Vrac, M., Stein, M., and Hayhoe, K.: Statistical downscaling of precipitation through nonhomogeneous stochastic weather typing, Clim. Res., 34, 169–184, doi:10.3354/cr00696, 2007. 4018

Wetterhall, F., Halldin, S., and Xu, C.-Y.: Statistical precipitation downscaling in central Sweden with the analogue method, J. Hydrol., 306, 174–190, doi:10.1016/j.jhydrol.2004.09.008, 2005. 4018, 4024

Wetterhall, F., Halldin, S., and Xu, C.-Y.: Seasonality properties of four statistical-downscaling methods in central Sweden, Theor. Appl. Climatol., 87, 123–137, doi:10.1007/s00704-005-0223-3, 2007. 4024

Wickham, H.: Reshaping data with the reshape package, available at: http://www.jstatsoft.org/v21/i12, J. Stat. Softw., 21, 1–20, 2007. 4028

Wickham, H.: ggplot2: elegant graphics for data analysis, Use R!, Springer, New York, doi:10.1007/978-0-387-98141-3, 2009. 4028

Wilby, R. L. and Wigley, T. M. L.: Precipitation predictors for downscaling: observed and general circulation model relationships, Int. J. Climatol., 20, 641–661, 2000. 4024

Wilby, R. L., Hassan, H., and Hanaki, K.: Statistical downscaling of hydrometeorological variables using general circulation model output, J. Hydrol., 205, 1–19, doi:10.1016/S0022-1694(97)00130-3, 1998. 4019

Zeileis, A. and Grothendieck, G.: Zoo: S3 infrastructure for regular and irregular time series, available at: http://www.jstatsoft.org/v14/i06/, J. Stat. Softw., 14, 1–27, 2005. 4029

Zhang, F. and Georgakakos, A. P.: Joint variable spatial downscaling, Climatic Change, 111, 945–972, doi:10.1007/s10584-011-0167-9, 2012. 4018

HESSD
10, 4015–4061, 2013

Table 1. Predictors and their corresponding pressure levels, times, similarity criterion and number of situations selected in the given step used by the downscaling method. E.d.: Euclidean distance, TWS: The Teweles and Wobus shape criteria (Teweles and Wobus, 1954).

Predictor	Pressure level [hPa] and time [UTC]	Similarity citerion	Number of analogues
Temperature	925 at 12:00 D+1, 600 at 12:00 D	E.d.	2000*
Geopotential	1000 at 12:00 D, 500 at 00:00 D+1	TWS	170
Vertical velocity	850 at 06:00, 12:00, 18:00 D and 00:00 D+1	E.d.	70
Humidity (TCW × rh)	850 at 12:00 D and 00:00 D+1	E.d.	25

*depending on the length of the archive: 100× number of years in the archive (44 yr → 4400, 20 yr → 2000, . . .).

HESSD
10, 4015–4061, 2013

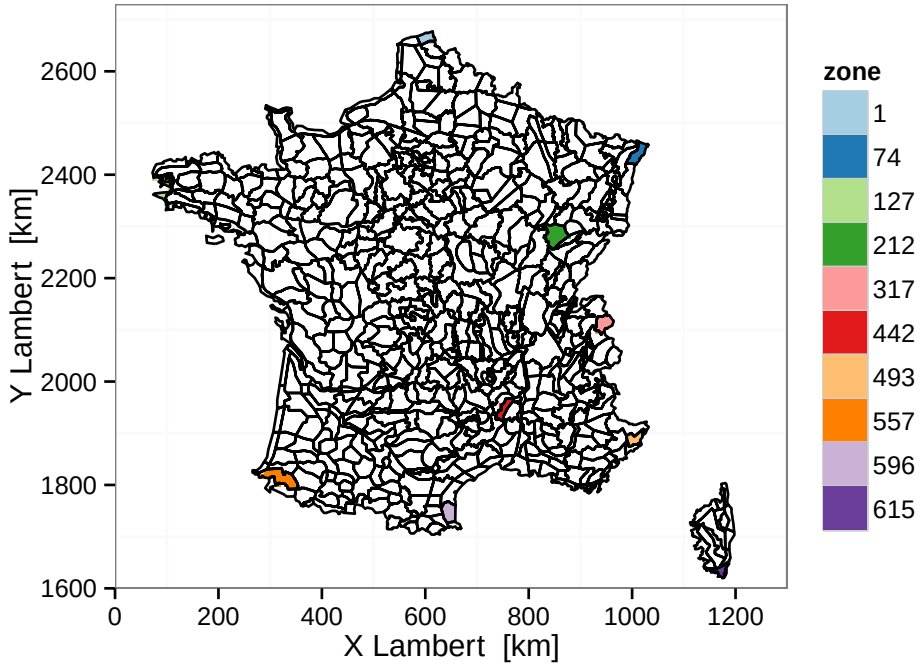

Fig. 1. The 608 climatologically homogeneous zones defined in the Safran data. The case study zones used in this study are colored. The three zones situated in the Rhône catchment are Saône (212, dark green), Arve (317, light red) and Ardèche (442, dark red). The seven zones located at the geographical limits of the country are shown with other colours.

HESSD
10, 4015–4061, 2013

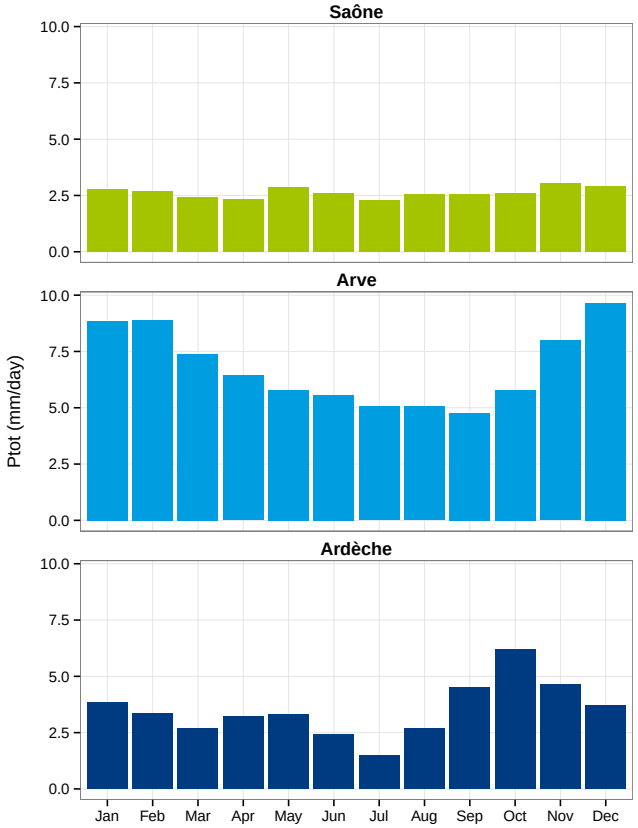

Fig. 2. Monthly mean precipitation, 1 August 1958–31 July 2002, from the Safran data for the three case study zones Saône, Arve and Ardèche.

HESSD
10, 4015–4061, 2013

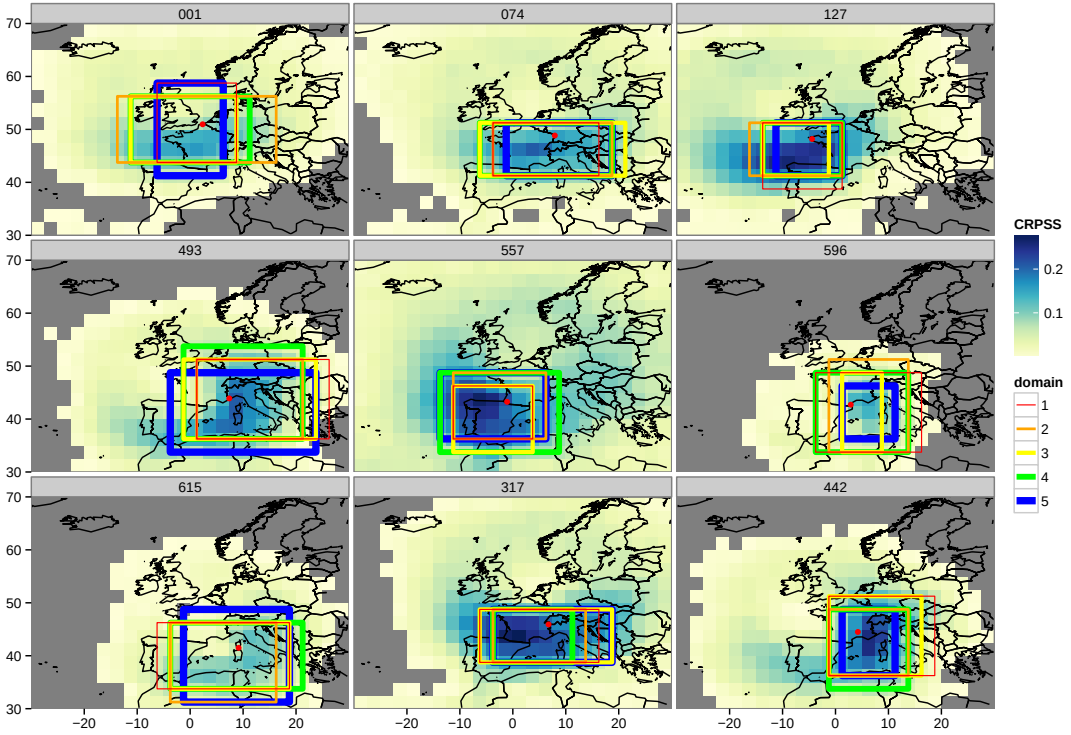

Fig. 3. Relevance maps truncated at CRPSS = 0 (regions with higher skill than the climatology) and optimised domains for nine zones using the 20 yr archive. The best domain found is drawn in red followed by the orange, yellow, green and blue one. The zone location is indicated by a red dot.

HESSD
10, 4015–4061, 2013

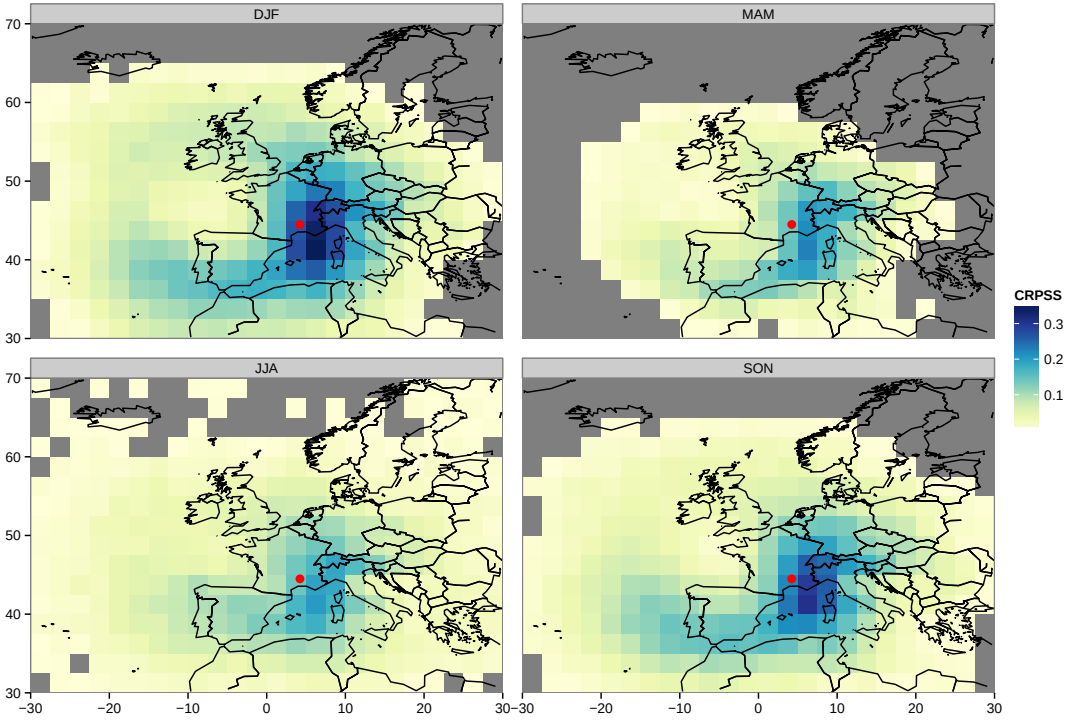

Fig. 4. Seasonal relevance maps for the Ardèche case study zone.

HESSD
10, 4015–4061, 2013

Optimising predictor domains for precipitation downscaling

S. Radanovics et al.

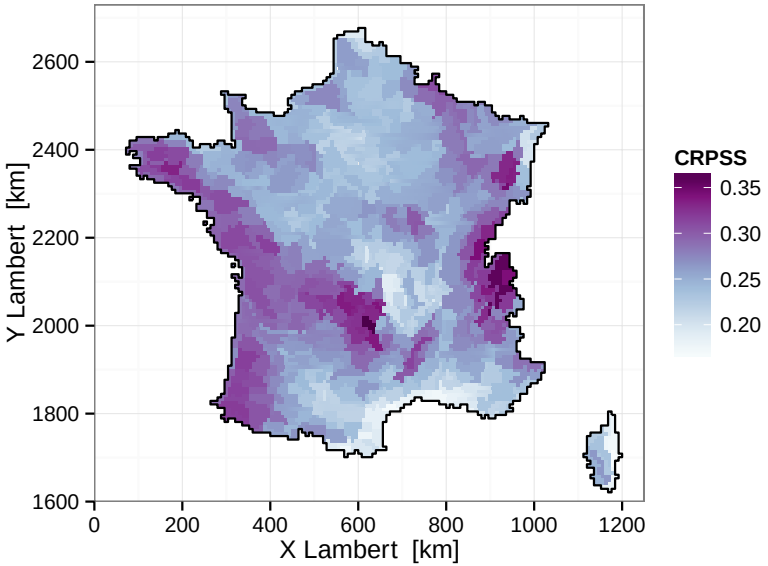

Fig. 5. Average CRPSS obtained with the best domains found during optimisation.

HESSD
10, 4015–4061, 2013

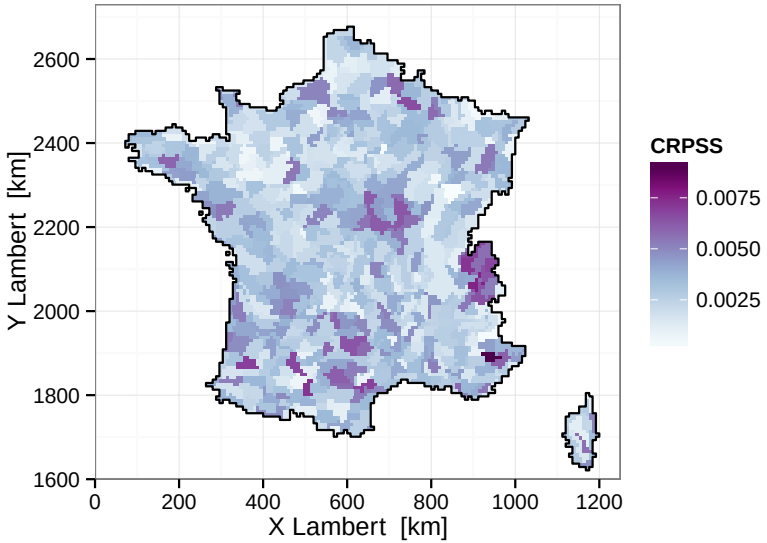

Fig. 6. Difference in CRPSS between the best and the 5th best domain found during optimisation.

HESSD
10, 4015–4061, 2013

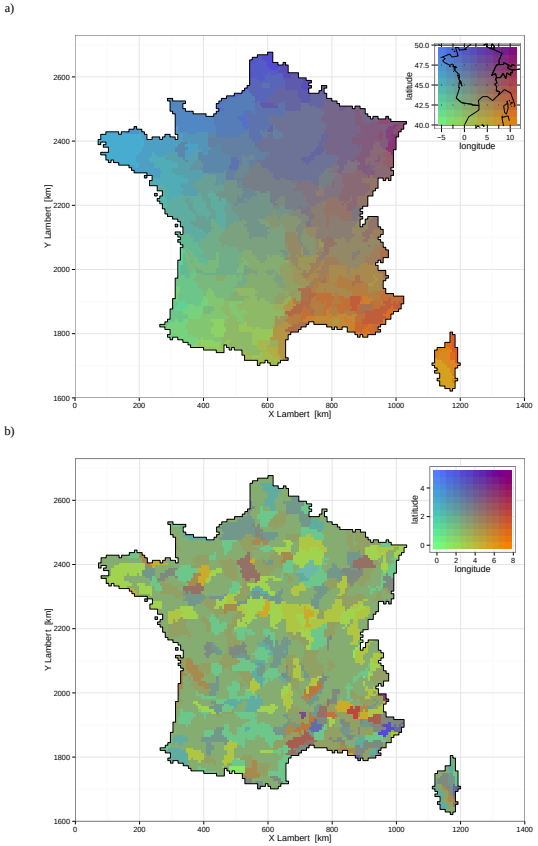

Fig. 7. (a) Mean domain center of the five best domains found during the domain optimisation. **(b)** Maximum difference in domain center location between two domains in the five best domain ensemble.

HESSD
10, 4015–4061, 2013

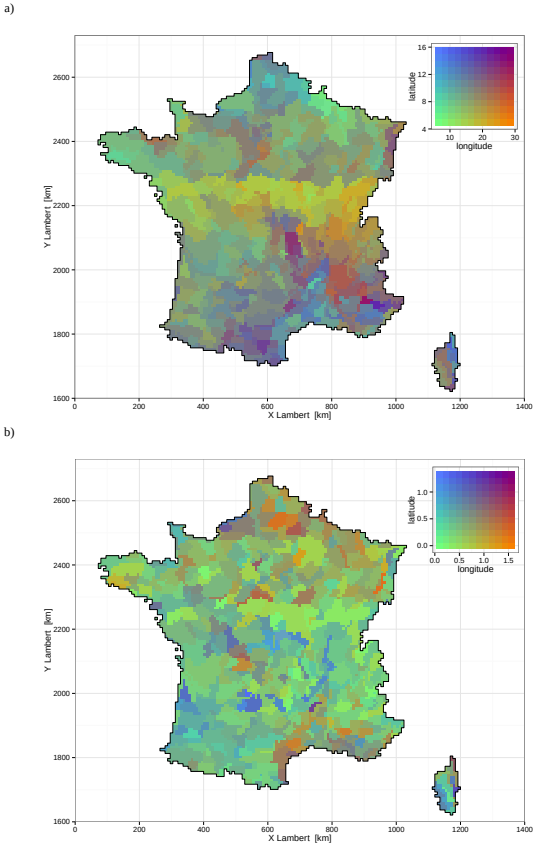

Fig. 8. (a) Mean domain size of the five best domains found during the optimisation procedure for each zone. **(b)** Ratio of domain size range in the five domain ensemble (range/mean size).

HESSD
10, 4015–4061, 2013

Optimising predictor domains for precipitation downscaling

S. Radanovics et al.

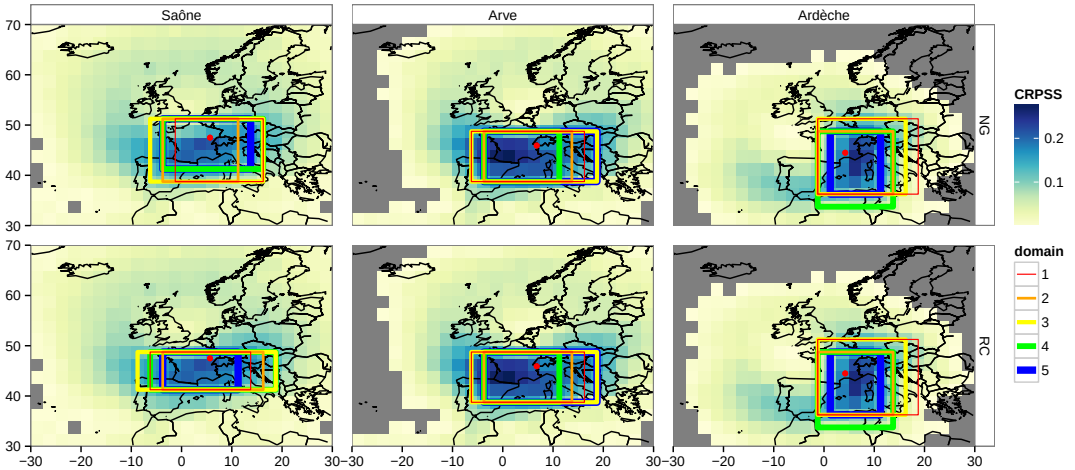

Fig. 9. Optimised predictor domains for three case study zones and different starting domains for the optimisation. First row: start at the nearest elementary domain (NG), second row: start from the most relevant elementary domain (RC).

HESSD
10, 4015–4061, 2013

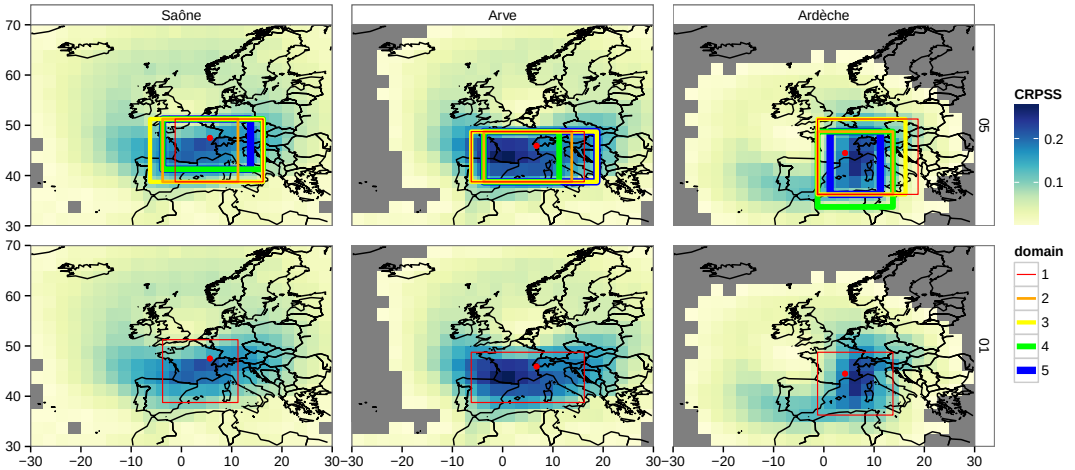

Fig. 10. Optimised predictor domains for three case study zones using the extended optimisation method with five domains (first row) or the basic optimisation method with one domain (second row).

HESSD
10, 4015–4061, 2013

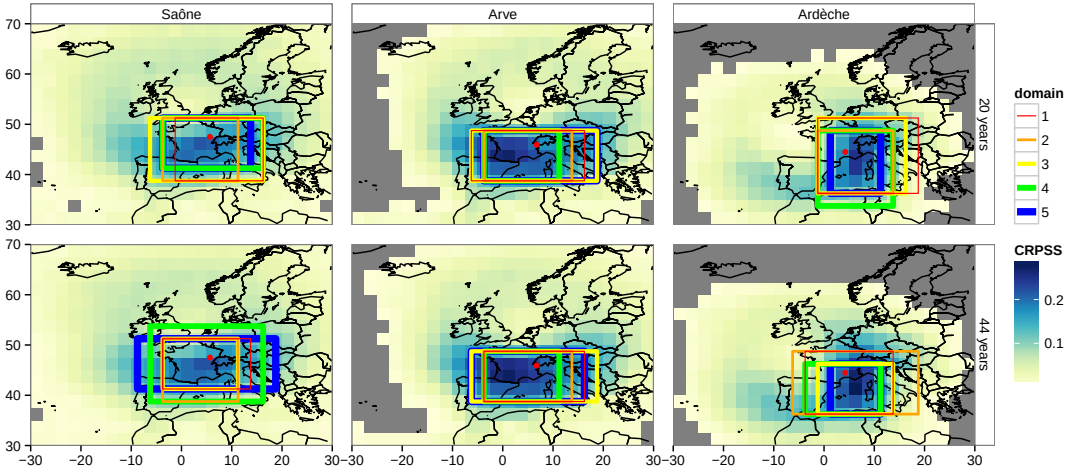

Fig. 11. Optimised predictor domains for three case study zones using 20 yr (first row) and 44 yr (second row) archive for optimisation.

HESSD
10, 4015–4061, 2013